

Multiphoton Dissociation of Transition-Metal Carbonyl Complexes: A Novel Route to Gas-Phase Metal Clusters

D. G. Leopold and V. Vaida*†

Contribution from the Department of Chemistry, Harvard University, Cambridge, Massachusetts 02138. Received March 7, 1983

Abstract: UV/visible multiphoton dissociation/ionization of a variety of transition-metal carbonyl complexes yields highly unsaturated metal-containing molecular ions in addition to atomic metal ions. Results demonstrate that photodissociation of stable metal carbonyl compounds provides a versatile, target-specific method of producing gas-phase samples of bare homonuclear and heteronuclear metal dimers and trimers, metal sulfides, and monoligated metal atoms.

We report here the production of gas-phase transition-metal clusters by UV/visible multiphoton dissociation (MPD) of volatile metal carbonyl compounds.¹ Due to the difficulty of producing gaseous samples of bare metal clusters, metal sulfides, and other structurally simple transition-metal systems, the spectroscopic data needed to test results of the current surge of theoretical efforts² are often not available. This is strikingly illustrated by a very recent report by Cotton and Shim of *ab initio* calculations on Ru₂.^{2a} This molecule, chosen as a particularly tractable theoretical subject,^{2a} has not yet proved tractable experimentally: there are no spectroscopic studies of Ru₂ in the literature, and even high-temperature equilibrium measurements of the dissociation energy are unavailable. The difficulties encountered in producing gas-phase samples of this highly refractory molecule by conventional methods are avoided by use of the metal carbonyl MPD technique reported here. This is illustrated by the production of dimers as well as trimers of ruthenium by photolysis of Ru₃(CO)₁₂, a stable, commercially available compound.

MPD of transition-metal carbonyls has several unique advantages over alternative³ metal cluster generation methods. For example, gas-phase clusters of refractory metals can be prepared without the use of high-temperature ovens. This is dramatically demonstrated here by the production of gaseous dimers and trimers of osmium (mp ~3000 °C) by photodissociation of Os₃(CO)₁₂ sublimed from a 120 °C source. In addition, dissociation of photolabile ligands from structurally well-defined precursors provides access to clusters of specific compositions. For example, MPD of carbonyl complexes containing heteronuclear metal cluster cores is employed here to generate iron-ruthenium dimers without detectable homonuclear dimer production, a difficult task for atom aggregation methods. Clearly, its ability to provide specific access to selected clusters renders this technique of immense potential value for studies employing non-mass-selective detection methods. The diversity of metal carbonyl compounds available,⁴ combined with the remarkable efficiency of multiphoton dissociation for producing highly unsaturated metal fragments from stable organometallic complexes,⁵ suggests the potential of the MPD technique for preparing a wide variety of well-defined gas-phase transition-metal clusters in sufficient concentrations for spectroscopic and chemical characterization.

Experimental Section

In these experiments, the gas-phase organometallic sample is photodissociated and the fragments are detected by multiphoton ionization mass spectrometry. A block diagram of the apparatus is shown in Figure 1. The solid sample is sublimed at 25–125 °C in a resistively heated stainless steel cylinder located inside a vacuum chamber maintained at 10⁻⁶ torr by a baffled 4-in. diffusion pump. The sample effuses through an orifice 1 mm in diameter and 4 cm from the region in which the mutually orthogonal sample source axis, laser beam, and mass spectrometer axis intersect. In the interaction region, the estimated sample number density is 10¹¹ molecules cm⁻³. A 1-mm collimator located 1 cm from the oven orifice prevents condensation of the heated sample on the mass spectrometer elements. The focussed beam of an excimer-pumped

dye laser system (Lambda Physik EMG101/FL2000) is used to irradiate the sample, and absorptions of several photons during a single 10-ns laser pulse result in sample dissociation and fragment ionization. In the experiments reported here, laser energies of 0.3–2 mJ and wavelengths between 385 and 500 nm were employed. A 20 cm focal length lens positioned 26 cm from the interaction region focussed the laser beam to 1 × 10⁻³ cm² there, producing fluxes of 10⁷–10⁸ W cm⁻².

A time-of-flight mass spectrometer was constructed for these studies in view of its ability to measure an entire photofragment mass spectrum following each laser pulse. The Wiley-McLaren design was chosen because the flexibility introduced by two acceleration regions affords optimum mass resolution while permitting convenient adjustment of the instrument.⁶ Photoions formed in the first acceleration region are directed along the mass spectrometer axis by a repeller plate positively biased with respect to a parallel grid (Buckbee-Mears 90% transmission, 70 wires/in. nickel electroformed mesh). Ions gain additional kinetic energy in a second acceleration region and then enter a field free drift region, through which their transit times vary according to their mass-to-charge ratios. The ion current is amplified by a Channeltron electron multiplier (Galileo 4830) and a fast ×100 preamplifier (Pacific Precision Instruments 2A50) and recorded as a function of transit time by a LeCroy WD8256 transient digitizer. System parameters were chosen to afford a mass resolution of ~100 for room-temperature ions while producing flight time distributions compatible with the 50-ns resolution of the transient digitizer. It was found that these requirements could be satisfied with optimum ion detection efficiency with use of a drift region ~50 cm in length and a total acceleration potential of ~600 V, producing ion flight times of ~1.6 (m/e)^{1/2} μs.

Data collection, display, and storage as well as synchronization of the experiment are performed by a Commodore PET microcomputer interfaced to the transient digitizer and to various digital and analog output ports, providing an effective yet notably inexpensive control system. The PET is programmed in 6502 microprocessor machine code to arm the digitizer, trigger the laser, acquire and sum data transferred from the digitizer, and provide real time video displays of individual and signal-averaged mass spectra. Data processing and storage functions allowing slower execution speeds are handled via a resident BASIC interpreter.

(1) A preliminary report of these results was presented at the Second International Conference on Photochemistry and Photobiology held in Alexandria, Egypt, January 5–11, 1983. Also see: V. Vaida, N. J. Cooper, R. J. Hemley, and D. G. Leopold, *J. Am. Chem. Soc.*, **103**, 7023 (1981).

(2) (a) F. A. Cotton and I. Shim, *J. Am. Chem. Soc.*, **104**, 7025 (1982). (b) M. M. Goodgame and W. A. Goddard, *Phys. Rev. Lett.*, **48**, 135 (1982). (c) D. A. Case, *Annu. Rev. Phys. Chem.*, **33**, 151 (1982). (d) M. C. Manning and W. C. Troglor, *Coord. Chem. Rev.*, **38**, 89 (1981).

(3) (a) D. L. Michalopoulos, M. E. Geusic, S. G. Hansen, D. E. Powers, and R. E. Smalley, *J. Phys. Chem.*, **86**, 3914 (1982). (b) V. E. Bondybe, G. P. Schwartz, and J. H. English, *J. Chem. Phys.*, **78**, 11 (1983). (c) Yu. M. Efremov, A. N. Samoilova, and L. V. Gurvich, *Chem. Phys. Lett.*, **44**, 108 (1976). (d) J. R. Blackborow and D. Young, "Metal Vapour Synthesis in Organometallic Chemistry", Springer-Verlag, Berlin, 1979, and references therein. (e) D. R. Preuss, S. A. Pace, and J. L. Gole, *J. Chem. Phys.*, **71**, 3553 (1979). (f) S. J. Riley, E. K. Parks, C.-R. Mao, L. G. Pobo, and S. Wexler, *J. Phys. Chem.*, **86**, 3911 (1982).

(4) (a) P. R. Raithby, in "Transition Metal Clusters", B. F. G. Johnson, Ed., John Wiley & Sons, Chichester, 1980. (b) P. Chini, G. Longoni, and V. G. Albano, *Adv. Organomet. Chem.*, **14**, 285 (1976). (c) W. L. Gladfelter and G. L. Geoffroy *ibid.*, **18**, 207 (1980).

(5) See ref 1 and references therein. Also see: (a) D. A. Lichtin, R. B. Bernstein, and V. Vaida, *J. Am. Chem. Soc.*, **104**, 1830 (1982). (b) S. Leutwyler and U. Even, *Chem. Phys. Lett.*, **84**, 188 (1981). (c) A. Gedanken, M. B. Robin, and N. A. Keubler, *J. Phys. Chem.*, **86**, 4096 (1982).

(6) (a) W. C. Wiley and I. H. McLaren, *Rev. Sci. Instrum.*, **26**, 1150 (1955). (b) G. Sanzoni, *ibid.*, **41**, 741 (1970).

† Alfred P. Sloan Fellow.

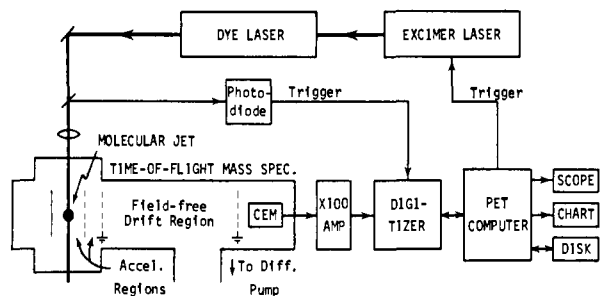


Figure 1. Block diagram of the apparatus. Elements defining the first and second acceleration regions of the time-of-flight mass spectrometer are separated by 1.50 and 1.00 cm, respectively. The repeller plate is biased at +663 V, the first acceleration grid is maintained at +550 V, and the two grids defining the 47.0 cm long drift region are grounded. The laser beam is focussed to a spot 0.4 mm in diameter and is centered in the first acceleration region. Additional details are given in the text. "CEM" denotes the channeltron electron multiplier, which was used to detect and amplify the ion current at a nominal gain of $\sim 10^6$.

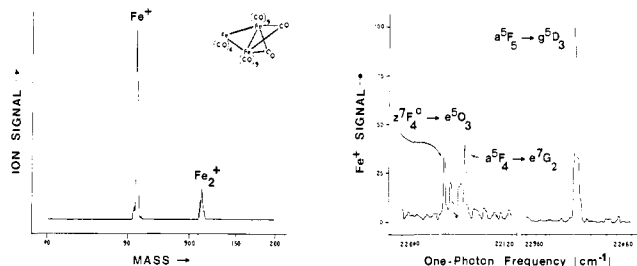


Figure 2. MPD/MPI of $\text{Fe}_3(\text{CO})_{12}$. The mass spectrum at left was obtained at 4500 \AA (22222 cm^{-1}) and $1 \times 10^8 \text{ W cm}^{-2}$. Scans to 1000 amu detected no additional ionic species. The MPI spectrum of Fe at right was obtained at 5-cm^{-1} resolution under the same experimental conditions. The lowest energy peak assigned is associated with a one-photon atomic transition, and the others with two-photon transitions. All of the assigned transitions originate from excited Fe levels and terminate at levels from which subsequent ionization requires the absorption of only one additional photon.

The system is generally operated at a laser repetition rate of 7 Hz, and results for 5000–10000 laser pulses are typically summed to produce a final mass spectrum. Multiphoton ionization (MPI) spectra of neutral fragments are obtained by scanning the dye laser and storing data from selected channels of the transient digitizer as a function of wavelength. This arrangement conveniently allows the MPI spectra of different ions to be monitored simultaneously during a single wavelength scan.

Pressure-dependence studies established that the molecular ions reported here were primarily formed as direct photoproducts rather than as products of combination reactions. In addition, atomic ion-molecule reactions were specifically ruled out as dominant mechanisms for molecular ion production by the dissimilar wavelength and flux dependences generally observed for atomic and molecular ions.

In the mass spectra reported here, laser wavelengths were chosen to avoid resonances with atomic transitions associated with strong MPI signal enhancements. Under these conditions, atomic ion signals were found to be roughly proportional to the laser pulse energy squared or cubed, while the production of molecular ions displayed a more linear I_0 dependence. The overall order of the MPD/MPI process in the systems studied is actually higher than these power dependences suggest (for example, production of Os^+ from $\text{Os}_3(\text{CO})_{12}$ at 385 nm requires the absorption of at least six photons), indicating the saturation of some steps in the multiphoton excitation process.

Results and Discussion

Figures 2–6 display mass spectra of ionic fragments formed by MPD/MPI of several transition-metal carbonyl complexes. The general path of photochemical behavior for metal carbonyls under UV/visible multiphoton excitation involves photodissociation followed by fragment ionization.^{5c,7} This contrasts with the

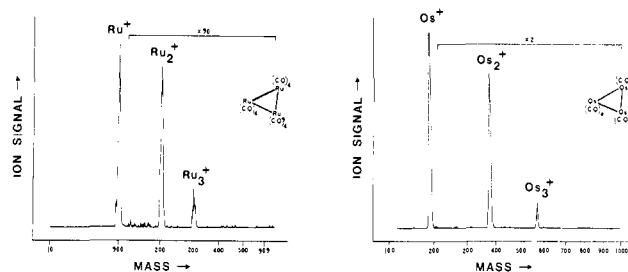


Figure 3. MPI mass spectra of $\text{Ru}_3(\text{CO})_{12}$ and $\text{Os}_3(\text{CO})_{12}$ at 385 nm. These spectra were obtained with use of source temperatures of 120°C and laser intensities of $2 \times 10^8 \text{ W cm}^{-2}$.

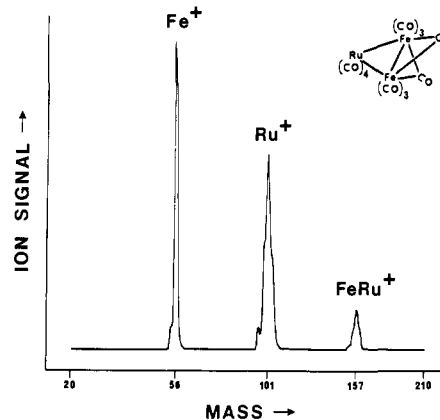


Figure 4. $\text{Fe}_2\text{Ru}(\text{CO})_{12}$ MPI mass spectrum at 385 nm. The bare trinuclear cluster Fe_2Ru^+ (213 amu) was also observed, at about 5% the intensity of FeRu^+ .

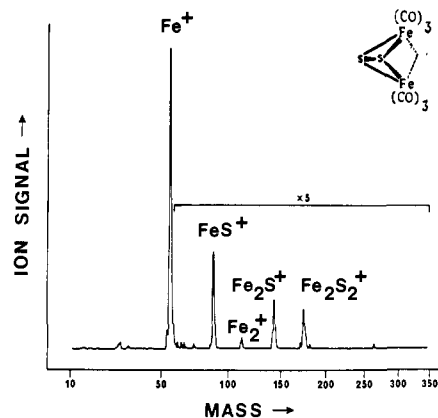


Figure 5. MPI mass spectrum of $\text{Fe}_2(\text{CO})_9\text{S}_2$ sublimed at room temperature and photolyzed at 385 nm, $1 \times 10^8 \text{ W cm}^{-2}$. FeS_2^+ was also observed in other runs employing higher laser fluxes.

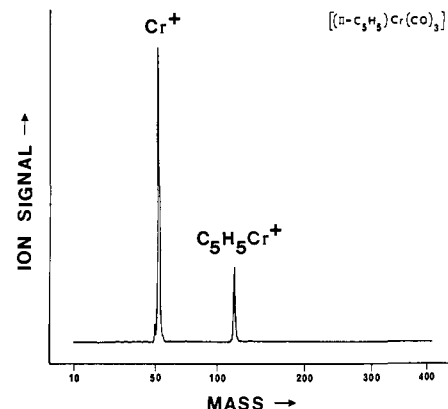


Figure 6. MPI mass spectrum of $[(\pi\text{-C}_5\text{H}_5)\text{Cr}(\text{CO})_3]_2$ at 385 nm, $4 \times 10^7 \text{ W cm}^{-2}$. CrCO^+ was not observed under these conditions, indicating an abundance $< 1\%$ that of $\text{C}_5\text{H}_5\text{Cr}^+$.

(7) (a) L. J. Rothberg, D. P. Gerrity, and V. Vaida, *J. Chem. Phys.*, **74**, 2218 (1981). (b) D. P. Gerrity, L. J. Rothberg, and V. Vaida, *Chem. Phys. Lett.*, **74**, 1 (1980). (c) Z. Karny, R. Naaman, and R. N. Zare, *ibid.*, **59**, 33 (1978).

Table I. Metal-Cluster Ions Detected by MPI-Mass Spectrometry of Photodissociated Transition-Metal Carbonyl Complexes

ion	precursors	ion	precursors
homonuclear metal clusters		heteronuclear metal clusters	
Mn ₂ ⁺	Mn ₂ (CO) ₁₀	FeRu ⁺	Fe ₂ Ru(CO) ₁₂ , FeRu ₂ (CO) ₁₂
Fe ₂ ⁺	Fe ₂ (CO) ₆ S ₂ , Fe ₃ (CO) ₁₂	Fe ₂ Ru ⁺	Fe ₂ Ru(CO) ₁₂
Co ₂ ⁺	Co ₂ (CO) ₈ , Co ₄ (CO) ₁₂	FeRu ₂ ⁺	FeRu ₂ (CO) ₁₂
Ru ₂ ⁺	FeRu ₂ (CO) ₁₂ , Ru ₃ (CO) ₁₂		
Ru ₃ ⁺	Ru ₃ (CO) ₁₂	metal-nonmetal clusters	
Re ₂ ⁺	Re ₂ (CO) ₁₀	MCO ⁺	Cr(CO) ₆ , Mn ₂ (CO) ₁₀
Os ₂ ⁺	Os ₃ (CO) ₁₂	C ₅ H ₅ Cr ⁺	[(π-C ₅ H ₅)Cr(CO) ₃] ₂
Os ₃ ⁺	Os ₃ (CO) ₁₂	MnBr ⁺	Mn(CO) ₅ Br
		Fe _{1,2} S _{1,2} ⁺	Fe ₂ (CO) ₆ S ₂

multiphoton photochemistry of many organic systems, which proceeds via initial ionization of the parent molecule and subsequent fragmentation to smaller ions.^{5c,8} Results shown in Figure 2 for MPD/MPI of Fe₃(CO)₁₂ illustrate the photoprocesses typical of the systems studied here. As seen in the mass spectrum at left, both atomic- and dimeric-metal ions were detected following 4500-Å excitation at 1×10^8 W cm⁻². The spectrum at right, obtained under the same experimental conditions, displays the wavelength dependence of Fe⁺ ion signal intensity in this spectral region. The pronounced peaks observed are associated with laser frequencies one- or two-photon resonant with allowed electronic transitions of the neutral metal atom.⁹ The background ion signal can be attributed to various processes, including molecular ion dissociation and other pathways to Fe⁺ not proceeding via the neutral atom. The relative weakness of this background signal indicates that such dissociative processes constitute at most minor mechanisms for Fe⁺ production, even under the photolysis conditions employed here which generate relatively large amounts of Fe₂⁺. In view of the known multiphoton photochemical behavior of metal carbonyls, MPI mass spectrometric detection of the metal-cluster fragment ions reported below can be viewed as strong although indirect evidence for the generation of the corresponding neutral metal clusters by multiphoton dissociation of the parent molecule.

Figure 3 illustrates the production of the bare homonuclear dimers and trimers of ruthenium and osmium by photodissociation of Ru₃(CO)₁₂ and Os₃(CO)₁₂ at 3853 Å. In the MPD cluster generation technique, the size of the metal core in the precursor molecule places an upper limit on the sizes of accessible bare clusters, enabling the observed production of metal trimers without the generation of tetramers or larger clusters. In contrast, the synthesis of trimers or larger bare-metal targets by atom aggregation methods is generally accompanied by the production of relatively large amounts of higher oligomers. These can complicate mass spectrometric studies by undergoing fragmentation processes resulting in stray signals at the mass of the target cluster, as well as introducing obvious difficulties in studies using non-mass-selective detection methods. An impressive array of bare homonuclear metal clusters is potentially accessible by the MPD technique: metal cluster carbonyl complexes containing up to six metal atoms are commercially available,¹⁰ and the syntheses and crystallographic characterizations of neutral compounds containing up to twelve metal atoms have been reported in the literature.⁴

(8) R. B. Bernstein, *J. Phys. Chem.*, **86**, 1178 (1982).

(9) C. E. Moore, *Natl. Bur. Stand. (U.S.), Circ.*, No. 467 (1952).

(10) For example, a wide variety of metal cluster carbonyl and carbonyl derivative compounds are available from Strem Chemicals, Inc. (P.O. Box 108, Newburyport, MA 01950) and from Pressure Chemical (3419 Smallman St., Pittsburgh, PA 15201).

The potential target specificity of the MPD cluster generation technique is further illustrated in Figure 4 by the observation of the heteronuclear ion FeRu⁺ as the only metal dimer detected following MPD/MPI of Fe₂Ru(CO)₁₂ with use of 3853 Å, 2×10^8 W cm⁻² excitation. The bare clusters Fe₂Ru⁺ and FeRu₂⁺ were also observed under these photolysis conditions from Fe₂Ru(CO)₁₂ and FeRu₂(CO)₁₂ precursors, respectively, and were in each case the only trinuclear clusters detected. Clearly, this degree of control over molecular composition is difficult to obtain by heteronuclear cluster generation techniques involving the collisional recombinations of metal atoms.^{3b-d} The absence of detectable Fe₂⁺ following MPD/MPI of Fe₂Ru(CO)₁₂, indicating a maximum abundance of 3% relative to FeRu⁺, can be rationalized in terms of a greater dissociation energy for the iron-ruthenium than for the iron-iron bond. Such a relative bond strength ordering is suggested by the general observation that strengths of metal-metal bonds between atoms of the same subgroup tend to increase with increased involvement of heavier atoms.¹¹ Also consistent with this trend are the relative yields of bare metal trimer ions following photolysis of the M₃(CO)₁₂/MM'₂(CO)₁₂ series: the intensity of the M₃⁺ or MM'₂⁺ ion signal, measured with respect to the total dimer ion signal, was found to increase from below 1% for Fe₃(CO)₁₂ (from which no Fe₃⁺ was detected), to ~5% for Fe₂Ru(CO)₁₂ and FeRu₂(CO)₁₂, to 20–30% for Ru₃(CO)₁₂ and Os₃(CO)₁₂.

In addition to the bare homonuclear and heteronuclear metal clusters already discussed, a number of interesting metal-nonmetal clusters have been produced by the MPD technique. As shown in Figure 5, photolysis of Fe₂(CO)₆S₂ gives rise to the totally decarbonylated tetrameric iron-sulfur core as well as to smaller metal sulfides. Several types of monoligated metals have been observed, including the monocarbonyls CrCO⁺ and MnCO⁺ produced by photolyses of Cr(CO)₆ and Mn₂(CO)₁₀, respectively,¹² and the metal halide dimer MnBr⁺ by MPD/MPI of Mn(CO)₅Br. In addition, C₅H₅Cr⁺ was detected following photolysis of [(π-C₅H₅)Cr(CO)₃]₂, as shown in Figure 6. Such monoligated species are often considered as models for molecules adsorbed on metal surfaces, and have been the objects of numerous experimental and theoretical efforts.¹³

The diversity of metal clusters generated to date, summarized in Table I, demonstrates the applicability of multiphoton dissociation of transition-metal carbonyl compounds for the designed synthesis of a wide variety of gas-phase metal clusters.

Acknowledgment. We would like to thank Jim Fox and Professors N. J. Cooper, G. L. Geoffroy, and D. Seyferth for generously providing some of the compounds used in these studies. Financial support from the National Science Foundation is gratefully acknowledged.

Registry No. Mn₂(CO)₁₀, 10170-69-1; Fe₂(CO)₆S₂, 14243-23-3; Co₂(CO)₈, 10210-68-1; FeRu₂(CO)₁₂, 12388-68-0; Ru₃(CO)₁₂, 15243-33-1; Re₂(CO)₁₀, 14285-68-8; Os₃(CO)₁₂, 15696-40-9; Cr(CO)₆, 13007-92-6; Fe₃(CO)₁₂, 17685-52-8; Co₄(CO)₁₂, 17786-31-1; [(π-C₅H₅)Cr(CO)₃]₂, 12194-12-6; Fe₂Ru(CO)₁₂, 20468-34-2; Mn(CO)₅Br, 14516-54-2.

(11) (a) P. Chini, *Pure Appl. Chem.*, **23**, 489 (1970). (b) J. A. Connor, in "Transition Metal Clusters", B. F. G. Johnson, Ed., John Wiley & Sons, Chichester, 1980.

(12) Also see ref 5a and Fisanick et al. [G. J. Fisanick, A. Gedanken, T. S. Eichelberger, IV., N. A. Kuebler, and M. B. Robin, *J. Chem. Phys.*, **75**, 5215 (1981)].

(13) For example, see: A. E. Stevens, C. S. Feigerle, and W. C. Lineberger, *J. Am. Chem. Soc.*, **104**, 19 (1982), and references therein.